www.nature.com/mtm

ARTICLE

Hemodynamics of a hydrodynamic injection

Tsutomu Kanefuji[1], Takeshi Yokoo[1], Takeshi Suda[1], Hiroyuki Abe[1], Kenya Kamimura[1] and Dexi Liu[2]

The hemodynamics during a hydrodynamic injection were evaluated using cone beam computed tomography (CBCT) and fluoroscopic imaging. The impacts of hydrodynamic (5 seconds) and slow (60 seconds) injections into the tail veins of mice were compared using 9% body weight of a phase-contrast medium. Hydrodynamically injected solution traveled to the heart and drew back to the hepatic veins (HV), which led to liver expansion and a trace amount of spillover into the portal vein (PV). The liver volumes peaked at $165.6 \pm 13.3\%$ and $165.5 \pm 11.9\%$ of the original liver volumes in the hydrodynamic and slow injections, respectively. Judging by the intensity of the CBCT images at the PV, HV, right atrium, liver parenchyma (LP), and the inferior vena cava (IVC) distal to the HV conjunction, the slow injection resulted in the higher intensity at PV than at LP. In contrast, a significantly higher intensity was observed in LP after hydrodynamic injection in comparison with that of PV, suggesting that the liver took up the iodine from the blood flow. These results suggest that the enlargement speed of the liver, rather than the expanded volume, primarily determines the efficiency of hydrodynamic delivery to the liver.

INTRODUCTION

Hydrodynamic delivery (HD) is well established and has widely prevailed in gene delivery to the liver in rodents since reported by Liu *et al.*[1] and Zhang *et al.*[2] in 1999. HD employs a physical force that is derived from the rapid injection of a large volume of a DNA solution equal to 8–10% of the body weight (BW) within 5–10 seconds into the mouse tail vein. Due to its physical nature, the use of HD has been extended from the delivery of genes to RNA,[3,4] small molecules,[5,6] proteins,[5,7] viruses,[8–10] and even cells.[11] Moreover, as HD requires neither viral nor nonviral vectors, it is considered to be the safest means for human gene therapy.[12–14] The major challenge in the field is to develop a revised and clinically applicable procedure for hydrodynamic gene delivery.[15–23]

Efforts and progress have been made toward the clinical use of HD using large animal models, including rabbits,[15] pigs,[16–20] dogs,[21–23] and nonhuman primates.[24] Since a large injection volume for HD could induce life threatening heart and lung failure,[5,25] reducing the injection volume has been the focal point of research in the past few years. A common strategy for reducing the injection volume is a HD directly into the liver using a balloon catheter inserted into a corresponding vessel such as the hepatic vein (HV) under fluoroscopic guidance.[15–20] Since the circulation is a closed system, a systemic HD in mice by a tail vein injection should be reproducible, as has been previously demonstrated.[1,2] The injected solution remains in the body, and its physical impact depends solely on the injection volume and speed. Practically, however, a regional HD could result in the spread of the injected solution from the injection site to other areas and spill over through various vascular connections.[20,26,27]

To establish a regional HD for clinical use, knowledge about the hemodynamics of HD is necessary. Unfortunately, all the information in support of our current understanding on how HD works is from the observations made in animals with an open abdomen that must, therefore, have crucial effects on its hemodynamics.[20,26,28,29] The current study aims to demonstrate the hemodynamics of a systemic hydrodynamic injection, in detail, without surgical intervention by employing state of the art high-resolution imaging techniques. Our results suggest that the key determinant for a highly efficient HD is the expansion speed of the liver.

RESULTS

Time course of hydrodynamic flow spreading

The hydrodynamically injected flow spreading was visualized on two-dimensional lateral images under fluoroscopic observation (Figure 1). The injected contrast medium reached the heart directly through the inferior vena cava (IVC), followed by a retrograde flow surging into the HVs. After the major trunks of the HVs were filled with the contrast medium, the liver began to expand. The portal vein (PV) was recognized soon after the liver expansion took place and disappeared at the end of the injection. The fluoroscopic video images in both the lateral and supine positions were available (Supplementary Videos S1 and S2, respectively). Interestingly, the greatest visibility of the retrograde flow into the PV, judging by the image intensity, was much lower than that of the HV at any given time. In contrast, the slowly injected contrast medium sequentially

[1]Department of Gastroenterology and Hepatology, Graduate School of Medical and Dental Sciences, Niigata University, Niigata, Japan; [2]Department of Pharmaceutical and Biomedical Sciences, College of Pharmacy, University of Georgia, Athens, Georgia, USA Correspondence: T Suda (suda@med.niigata-u.ac.jp)
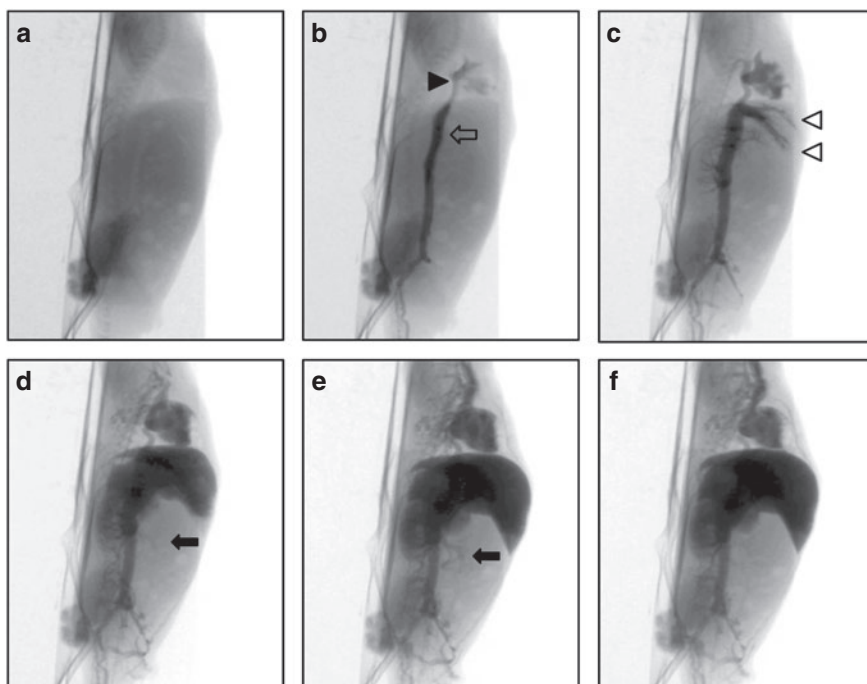
Figure 1   Solution spreading during a hydrodynamic injection. A continuous lateral view of the fluoroscopic images (**a–f**) was recorded during the entire course of the hydrodynamic injection. The contrast medium injected into the tail vein reached the heart first (closed arrowhead) *via* the inferior vena cava (open arrow) (**b**), followed by the retrograde flow surging into the hepatic veins (**c**, open arrowheads). Although the portal veins appeared to be visualized after the liver expansion took place (**d**, closed arrow) and gradually extended toward the periphery (**e**, closed arrow), as soon as the injection ended, the portal vein could no longer be recognized (**f**).

visualized the vasculature and organs in the order that the ante-grade flow was passing through. As shown in Supplementary Video S3, the kidneys, and then the liver became recognizable after the arterial system was visualized.

Liver expansion dynamics evoked by a hydrodynamic injection
Since a cone beam computed tomography (CBCT) requires ~3 minutes for the data acquisition to generate an image, a real-time observation of the liver structure in three dimensions could not be accomplished. However, the ventrodorsal fluoroscopic view of the liver was continuously recorded to assess the liver expansion during and after the HD using a 9% BW volume equivalent of the contrast medium in three mice. A virtual triangle was defined based on clearly identifiable anatomical structures to compare an area in the liver over time (Figure 2a), and the relative areas were evaluated quantitatively throughout the observation period, as shown in Figure 2b. When the area of each triangle was expressed as a percentage of the area at the earliest time point, the area continuously enlarged and peaked at the end of the injection, reaching $157.1 \pm 18.7\%$ (Figure 2b). After completing the injection, the area did not change significantly within the first 10 seconds.

Next, the ventrodorsal liver area was compared between the fluoroscopic and CBCT studies. Three-dimensional CBCT volumetric data were obtained after the above fluoroscopic study of three mice. As shown in Figure 3a, a ventrodorsal maximum intensity projection (MIP) of the liver CBCT images was strikingly similar to the fluoroscopic ventrodorsal liver image that was recorded at the end of the injection. The ventrodorsal liver areas that were deduced from the CBCT MIP were $99.2 \pm 2.2\%$ of these from the fluoroscopic images and were not significantly different from each other ($P = 0.61$, Figure 3b).

Finally, the liver volumes of the above three mice were calculated from the CBCT volumetric data and expressed as the relative liver volume to that of the control mice and were compared with those of the animals given the slow injection. The final liver volumes after the hydrodynamic and slow injections were $165.6 \pm 13.3\%$ and $165.5 \pm 11.9\%$ of the average volumes of the control mice and were not significantly different from each other ($P = 0.99$, Figure 3c).

Distribution difference of the solution between hydrodynamic and slow injections
As shown in Figure 4a, the image intensities were measured in five regions: the right atrium (#1), HV (#2), PV (#3), IVC caudal to the commissura of the HVs (IVC, #4), and the liver parenchyma (LP, #5) in the above three mice from each hydrodynamic or slow injection. As shown in Figure 4b, the image intensity of PV (median and inter-quartile range: 3536 and 3467—3590 Hounsfield unit (HU)) was significantly higher than that of LP (2844 and 2811—2975 HU, $P < 0.05$) in slow injection, whereas hydrodynamic injection resulted in a significantly higher intensity of LP (5255 and 5243—5622 HU) comparing with that of PV (2474 and 2428—2554 HU, $P < 0.05$). There were no significant differences in the image intensities between any other comparisons including between PV and HV. The CBCT MIP images represent the distribution of the contrast medium after both the hydrodynamic and slow injections (Figure 4b and Supplementary Videos S4 and S5).

DISCUSSION
Since its establishment in 1999, HD has gained wide acceptance as a tool for broader use in targeting the liver in gene therapy studies, the functional analysis of regulatory elements, the evaluation
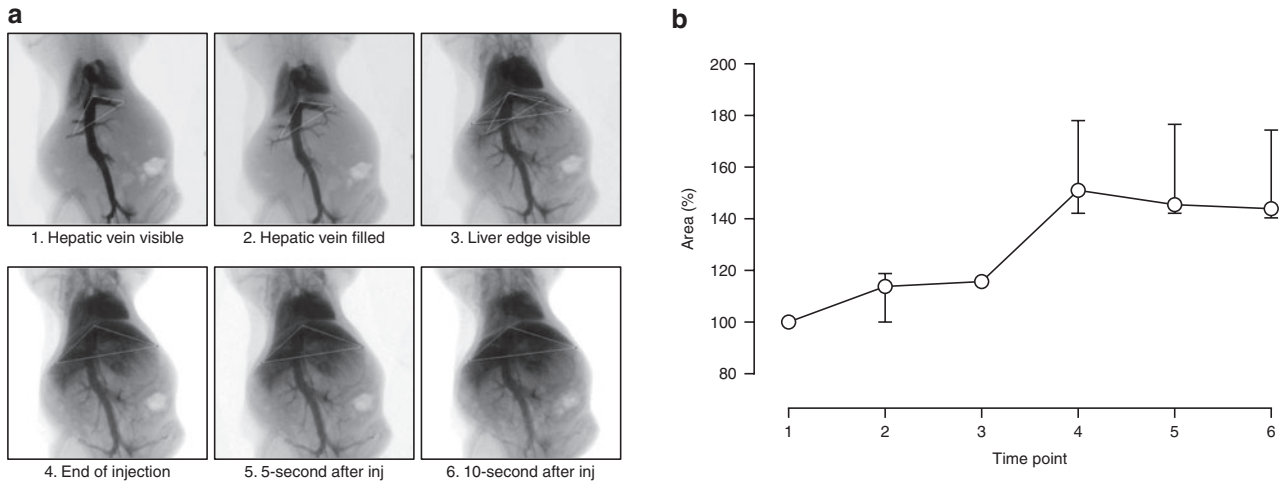
Figure 2 Transition of liver size and appearance during a hydrodynamic injection. (**a**) A triangle formed by three apexes, which were assigned as specific points of proximal branches of the hepatic veins, was defined as soon as they were visualized (time point 1) and was followed until the edge of the liver was revealed (time point 3). Another triangle was assigned using three apexes (time point 3) that were definitively determined at the edge of the liver and followed until 10 seconds after the end of the injection (time point 6). (**b**) The areas of the triangles at each time point were expressed as a value relative to the area at time point 1. The area of the second triangle was converted to a value relative to that of the first triangle on the basis of the areas at time point 3, when the areas could be measured for both triangles. The values were the median and the range calculated from three mice. Inj, injection.
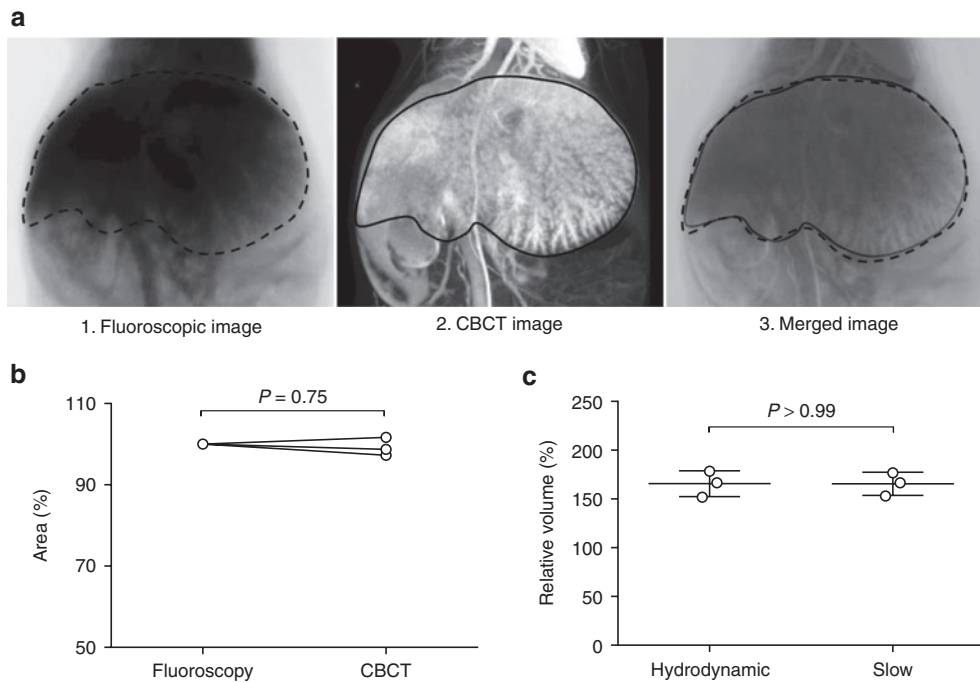

Figure 3 Enlargement of the liver volume. (**a**) The expansion of the liver was visualized during the course of a hydrodynamic injection in real-time under the fluoroscope, and the image immediately at the end of the injection was captured (1). Because respiration causes motion artifacts in cone beam computed tomography (CBCT), the mice underwent the CBCT scan immediately after euthanasia at the end of the injection. This provides a maximum intensity projection image based on the three-dimensional volumetric data (2). To clarify the effect of the time elapsed during the CBCT scan on the liver volume, both images were merged (3). The dotted and solid lines define the edge of the liver that was recognized in the fluoroscopic and CBCT images, respectively, of the same mouse in a supine position. (**b**) The areas of the entire liver that were calculated from the CBCT data were not significantly different from those based on the fluoroscopic images. (**c**) The entire liver volumes were significantly enlarged after the injection of the contrast medium with the 9% body weight volume, but they were not significantly different between the hydrodynamic ($165.6 \pm 13.3\%$) and the slow ($165.5 \pm 11.9\%$) injections. The volume is expressed as a percentage of the volume of 3 control mice in mean $\pm$ SD.

of gene products, and in RNAi studies in rodents.[12,30–32] The current practice in HD is guided by rich experimental results based on the structure and properties of blood capillaries as well as the dynamics of fluids passing through the vasculature.[18,20,26–29,31,33] However, the actual flow dynamics in HD have never been visualized in detail to understand the physical impact on the liver. The continuous capture of the fluoroscopic images in this study enabled us to follow the solution spreading with the resolution of 10 µm in space and 50 msec in time. In agreement with the insight from Liu *et al.*,[5] our results reveal that a solution splashed into the IVC after
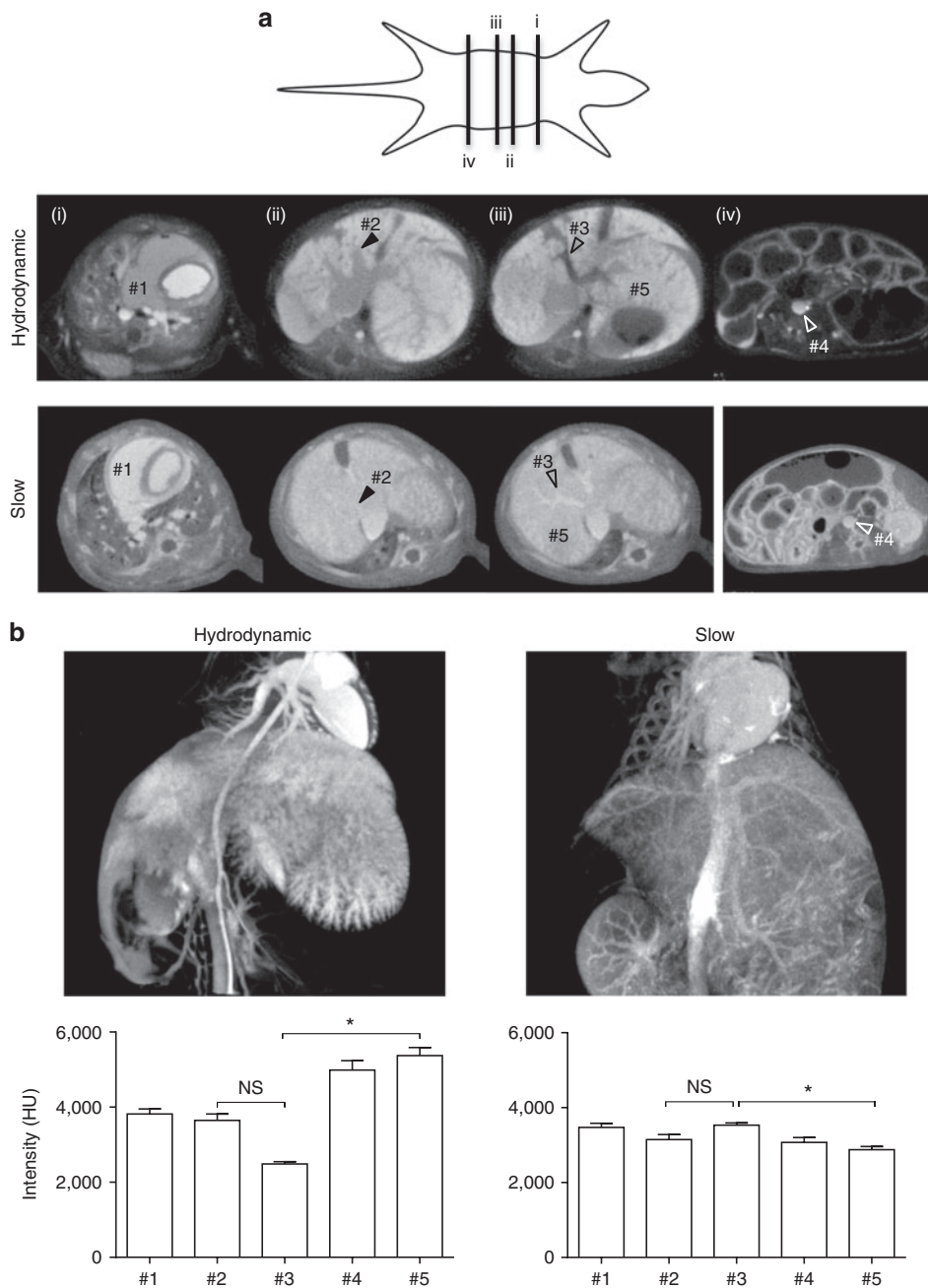
Figure 4 Distribution of the injected solution. (**a**) The mice were euthanized soon after either a hydrodynamic or slow injection of the phase-contrast medium (9% of body weight) into the tail vein, and underwent a cone beam computed tomography (CBCT) scan for the reconstruction of the slices (i–iv) suitable for the measurement of the image intensity. The intensities were measured at the right atrium (#1, RA), hepatic vein (#2, HV), portal vein (#3, PV), inferior vena cava caudal to the commissura of the hepatic veins (#4, IVC), and liver parenchyma (#5, LP). (**b**) Representative maximum intensity projection images showing the distribution of the contrast medium after the hydrodynamic and slow injections. The median intensities were higher at PV than at LP in the mice receiving a slow injection. In contrast, the intensities were significantly higher at LP than at PV in the mice receiving a hydrodynamic injection (*$P < 0.05$). There was no significant difference in the image intensity between other combinations including PV and HV. Three mice were used for each of the hydrodynamic and slow injections. The error bars indicate mean + SD.

a hydrodynamic tail vein injection hits the heart immediately and induces a powerful retrograde flow into the HVs toward the LP. On the other hand, although the orifice of the HV was detectable by the to-and-fro flow before the arterial system became visible, the HV itself was darkened following the enhancement of the liver, suggesting that an antegrade natural flow, not a retrograde flow, brought the contrast medium to the sinusoid of the liver during the slow injection.

Although massive backflow into the PV over the liver was suggested under open abdomen,[29] the drainage into the portal system was remarkably limited under natural conditions of both distance and volume (Figure 1d,e). This difference is likely because the large and small intestines must be dislocated from the abdominal cavity in an open abdomen to observe the portal flow during and after a hydrodynamic injection.[28] The dislocation of the intestines hampers the arterial blood supply to the intestines, which causes a reduction

in the natural portal flow. The expansion of the internal organs during a hydrodynamic injection raises the venous pressure and resistance against the backflow into the PV under natural conditions more readily than an open abdomen. Although the differences in the chemical properties between the contrast medium and normal saline may have hemodynamic effects, previous reports of massive backflow into the PV would have resulted from a surgically opened abdomen.[28,29] The results of the current study suggest that HD *via* the tail vein may not induce a critical backflow of the injected solution into the PV as long as the procedure is performed under natural conditions without open abdominal surgery.

Photogrammetry has revealed that the liver expands and reaches ~240% of its original size due to a hydrodynamic injection in mice[28] and swine.[20] Again, these observations come from open abdominal conditions. The entire liver expansion was expected from the restricted observational window of the dissected abdominal wall, where the liver can enlarge relatively easily with less resistance. However, under natural conditions, the abdominal cavity does not expand rapidly, but rather, restricts the volume expansion of the internal organs. Although the CBCT volumetric data could not be collected immediately after the injection when the liver reached its largest volume, a comparison of the ventrodorsal images revealed that the MIP of the CBCT data and the real-time view of the fluoroscopy were quite consistent with each other, suggesting that the liver volume deduced from the CBCT data could be used as a surrogate for the volume at the end of the injection. This is the first report of the volume change of the liver due to a hydrodynamic injection based on three-dimensional volumetric data.

Unexpectedly, the CBCT volumetric analyses revealed that there was no significant difference in the maximal liver volume between the hydrodynamic and slow injections. A previous photogrammetry study suggested that the liver reaches ~150% of its original volume after a 60-second injection of 9% BW equivalent of saline in mice,[28] less than the 165.5% that was suggested in this study. The intravenous injection of a large volume of solution into the IVC causes the exudation of bodily fluids from the capillaries. Actually, the contrast medium was observed in the abdominal cavity outside of the organs without any surgical procedures (data not shown). It is likely that the volume of the exudate increased in the open abdominal condition because of the damage to the tissues from the surgery. Therefore, the small reduction of the maximal volume of the liver is reasonable in a photogrammetric study in which the open abdominal observation is necessary. In contrast, the large difference (240% (ref. 28) versus 165.6%) between the open and closed abdomen injections suggests that the final expanded volume is not likely to be an exclusive determinant for gene delivery efficiency to the liver in HD. An open abdomen allows the liver to expand further than it would under natural conditions; however, it has been reported that the gene delivery efficiency between the closed and open abdominal conditions is not significantly different.[18,34,35] Although an optimal HD condition must be different between rodents and large animals, in which 250% of the original liver volume was proposed to be the best injection volume,[36] the volume of solution required to achieve the maximal delivery efficiency can be further reduced by adjusting key determinants. A report[36] has indicated that HD using a 250% liver volume was better than the injection of 125% and was similar to that of an injection using a 300% liver volume suggesting that the ideal volume would be between 125 and 250%.

Quantitative evaluation of the CBCT values over the body indicated that the hydrodynamically injected solution is trapped from the bloodstream into the liver tissues at the end of the injection.

Under hydrodynamic conditions, the blood containing the lowest amount of the contrast medium flowing into the liver *via* the PV mixed with the blood with the highest amount of contrast medium from the IVC distal to the liver and formed the same CBCT values in the HV and right atrium. Because the liver showed the highest CBCT values at that moment, the right atrium and HV would show similar CBCT values to those in the IVC if a significant amount of the contrast medium was washed out into the HV by the portal and hepatic arterial flows. Therefore, coupled with the capability of hydrodynamic force to deliver a wide variety of materials with different chemical properties, the immediate delivery strongly suggests that the physical impacts rather than those of a biological nature are the crucial determinants of HD.[37–39]

Because many physical factors cannot be completely dissociated from each other in a hydrodynamic injection, one might not be able to establish a single exclusive determinant for delivery efficiency. Thorough investigations have suggested that the injection speed, injection volume, static pressure in the liver, and shear stress are not single predominant factors. The combination of a high injection speed and a large injection volume is fundamental in HD. A quick injection or large volume alone cannot achieve maximal delivery efficiency. A quick injection using a small volume can quickly induce high pressure inside the liver, but the delivery efficiency is not comparable to that achieved under proper hydrodynamic conditions. When HD is performed in animals with a fibrotic liver, the pressure inside the liver rises rapidly to a higher pressure than that observed in animals with less liver fibrosis. The shear stress should be stronger in the fibrotic liver due to the rapid flow. A fibrotic liver expands less readily and there is less transgene expression.[40] With an open abdomen, the liver expansion is correlated with the delivery efficiency in any given circumstance. The current study, however, clearly shows that the expanded liver volume itself does not vary between the hydrodynamic and slow injections. Taken together, the current study suggests that the liver expansion rate would be a good surrogate for the gene delivery efficiency in a HD by consolidating the injection speed, injection volume, pressure inside the liver, shear stress and variety of anatomical structures, such as fibrosis. By ensuring a liver expansion rate that is within a certain range, a regional HD may be able to accomplish the safety and efficiency required for feasibility in clinical applications.

MATERIALS AND METHODS
Animals and imaging studies
All animal experiments were conducted in full compliance with regulation and approved by the Institutional Animal Care and Use Committee at the Niigata University. Female BALB/c mice (20–21 g) were purchased from Charles River Laboratories Japan. (Yokohama, Japan). Under anesthesia by the intraperitoneal injection of 4 mg of 2,2,2-tribromoethanol, a 24 G catheter (TERUMO, Tokyo, Japan) connected to a syringe filled with the contrast medium (Proscope, Bayer, Osaka, Japan) containing iodine at a concentration of 623.4 mg/ml, was inserted into the tail vein. The mouse was placed on the examination table in an R_mCT2 gantry (Rigaku Corporation, Tokyo, Japan) and injected with a 9% BW equivalent volume in either 5 (hydrodynamic injection) or 60 seconds (slow injection). For the fluoroscopic study, ventrodorsal or lateral images were obtained continuously every 50 msec from injection initiation to 10 seconds after the injection. To obtain three-dimensional volumetric data, a CBCT study was performed for a field of view of 30 mm using the current and voltage of 160 µA and 90 kV, respectively; this requires 26 seconds to collect the voxel data and ~2½ minutes to render 512 high-definition images with 10 µm pixels. After the fluoroscopic imaging, the mice were euthanized to avoid motion artifacts and the CBCT was performed immediately. To quantify the natural liver volume as a control, the mice were euthanized and underwent a CBCT after a slow injection of contrast medium with a dose of 1.5% BW taking 5 minutes to distinguish the liver edge.

Fluoroscopic two-dimensional quantification of liver deformation

To quantify the deformation of the liver due to the injection, a virtual triangle was defined in the liver by assigning three apexes based on anatomical structures. At the early stages of the injection, it was relatively easy to determine a branching point of the HVs adjacent to the IVC, while the liver edge rendered a distinct structure at the end of and after the injection, because the LP was clearly observed after the spread of the contrast medium into the sinusoid. Therefore, two virtual triangles were assigned in the images based on the HVs and the liver edges in the early and later observation periods, respectively, and both triangles were defined at the same time. By converting the area of the first triangle relative to the second, the area was quantified through the entire process using ImageJ software (version 1.6.0_51, National Institutes of Health, Bethesda, MD).

Conversion of voxel data to volume, intensity, and MIP

The area consisting of the LP was sequestrated in each transverse image of the CBCT by manually tracing an outline of the liver and its large vessels, such as the major trunks of the PVs, HVs, and IVC. The liver volume was calculated using OsiriX (version 3.9.4., Pixmeo, Geneva, Switzerland) at a scale of 2×10^{-4} mm^3 per voxel according to a method that is clinically well established for liver transplantation.[41,42] To compare a dose of the contrast medium in various regions over the body, the HU intensity of the images was measured three times for each region where air measures -1000 HU and water measures 0 HU. The MIP images were reconstructed using the 3D-MIP function of OsiriX.

Statistical analysis

The data are expressed as the median and interquartile range or the absolute number with percentages, as appropriate. Wilcoxon matched-pairs signed rank and Mann–Whitney tests were performed for comparisons of the areas between the fluoroscopic and CBCT studies and of the volumes between the hydrodynamic and slow injections. A comparison of the image intensities between the various regions was performed using Kruskal–Wallis followed by Dunn's multiple comparisons *post hoc* tests. All the statistical analyses were performed using GraphPad Prism version 6.0 (GraphPad Software, La Jolla, CA), and two-sided *P* values of less than 0.05 were considered statistically different.

REFERENCES

1   Liu, F, Song, Y and Liu, D (1999). Hydrodynamics-based transfection in animals by systemic administration of plasmid DNA. *Gene Ther* **6**: 1258–1266.

2   Zhang, G, Budker, V and Wolff, JA (1999). High levels of foreign gene expression in hepatocytes after tail vein injections of naked plasmid DNA. *Hum Gene Ther* **10**: 1735–1737.

3   McCaffrey, AP, Meuse, L, Pham, TT, Conklin, DS, Hannon, GJ and Kay, MA (2002). RNA interference in adult mice. *Nature* **418**: 38–39.

4   Lewis, DL, Hagstrom, JE, Loomis, AG, Wolff, JA and Herweijer, H (2002). Efficient delivery of siRNA for inhibition of gene expression in postnatal mice. *Nat Genet* **32**: 107–108.

5   Zhang, G, Gao, X, Song, YK, Vollmer, R, Stolz, DB, Gasiorowski, JZ *et al.* (2004). Hydroporation as the mechanism of hydrodynamic delivery. *Gene Ther* **11**: 675–682.

6   Kobayashi, N, Nishikawa, M, Hirata, K and Takakura, Y (2004). Hydrodynamics-based procedure involves transient hyperpermeability in the hepatic cellular membrane: implication of a nonspecific process in efficient intracellular gene delivery. *J Gene Med* **6**: 584–592.

7   Kobayashi, N, Kuramoto, T, Yamaoka, K, Hashida, M and Takakura, Y (2001). Hepatic uptake and gene expression mechanisms following intravenous administration of plasmid DNA by conventional and hydrodynamics-based procedures. *J Pharmacol Exp Ther* **297**: 853–860.

8   Brunetti-Pierri, N, Palmer, DJ, Mane, V, Finegold, M, Beaudet, AL and Ng, P (2005). Increased hepatic transduction with reduced systemic dissemination and proinflammatory cytokines following hydrodynamic injection of helper-dependent adenoviral vectors. *Mol Ther* **12**: 99–106.

9   Condiotti, R, Curran, MA, Nolan, GP, Giladi, H, Ketzinel-Gilad, M, Gross, E *et al.* (2004). Prolonged liver-specific transgene expression by a non-primate lentiviral vector. *Biochem Biophys Res Commun* **320**: 998–1006.

10   Arad, U, Zeira, E, El-Latif, MA, Mukherjee, S, Mitchell, L, Pappo, O *et al.* (2005). Liver-targeted gene therapy by SV40-based vectors using the hydrodynamic injection method. *Hum Gene Ther* **16**: 361–371.

11   Li, J, Yao, Q and Liu, D (2011). Hydrodynamic cell delivery for simultaneous establishment of tumor growth in mouse lung, liver and kidney. *Cancer Biol Ther* **12**: 737–741.

12   Kamimura, K and Liu, D (2008). Physical approaches for nucleic acid delivery to liver. *AAPS J* **10**: 589–595.

13   Suda, T, Kamimura, K, Kubota, T, Tamura, Y, Igarashi, M, Kawai, H *et al.* (2009). Progress toward liver-based gene therapy. *Hepatol Res* **39**: 325–340.

14   Kamimura, K, Suda, T, Zhang, G and Liu, D (2011). Advances in Gene Delivery Systems. *Pharmaceut Med* **25**: 293–306.

15   Eastman, SJ, Baskin, KM, Hodges, BL, Chu, Q, Gates, A, Dreusicke, R *et al.* (2002). Development of catheter-based procedures for transducing the isolated rabbit liver with plasmid DNA. *Hum Gene Ther* **13**: 2065–2077.

16   Yoshino, H, Hashizume, K and Kobayashi, E (2006). Naked plasmid DNA transfer to the porcine liver using rapid injection with large volume. *Gene Ther* **13**: 1696–1702.

17   Aliño, SF, Herrero, MJ, Noguera, I, Dasí, F and Sánchez, M (2007). Pig liver gene therapy by noninvasive interventionist catheterism. *Gene Ther* **14**: 334–343.

18   Suda, T, Suda, K and Liu, D (2008). Computer-assisted hydrodynamic gene delivery. *Mol Ther* **16**: 1098–1104.

19   Fabre, JW, Grehan, A, Whitehorne, M, Sawyer, GJ, Dong, X, Salehi, S *et al.* (2008). Hydrodynamic gene delivery to the pig liver via an isolated segment of the inferior vena cava. *Gene Ther* **15**: 452–462.

20   Kamimura, K, Suda, T, Xu, W, Zhang, G and Liu, D (2009). Image-guided, lobe-specific hydrodynamic gene delivery to swine liver. *Mol Ther* **17**: 491–499.

21   Zhang, G, Vargo, D, Budker, V, Armstrong, N, Knechtle, S and Wolff, JA (1997). Expression of naked plasmid DNA injected into the afferent and efferent vessels of rodent and dog livers. *Hum Gene Ther* **8**: 1763–1772.

22   Su, LT, Gopal, K, Wang, Z, Yin, X, Nelson, A, Kozyak, BW *et al.* (2005). Uniform scale-independent gene transfer to striated muscle after transvenular extravasation of vector. *Circulation* **112**: 1780–1788.

23   Hackett, PB, Aronovich, EL, Hunter, D, Urness, M, Bell, JB, Kass, SJ *et al.* (2013). Efficacy and safety of sleeping beauty transposon-mediated gene transfer in preclinical animal studies. *Curr Gene Ther* **11**: 612–625.

24   Zhang, G, Budker, V, Williams, P, Subbotin, V and Wolff, JA (2001). Efficient expression of naked dna delivered intraarterially to limb muscles of nonhuman primates. *Hum Gene Ther* **12**: 427–438.

25   Sawyer, GJ, Dong, X, Whitehorne, M, Grehan, A, Seddon, M, Shah, AM *et al.* (2007). Cardiovascular function following acute volume overload for hydrodynamic gene delivery to the liver. *Gene Ther* **14**: 1208–1217.

26   Sawyer, GJ, Zhang, X and Fabre, JW (2010). Technical requirements for effective regional hydrodynamic gene delivery to the left lateral lobe of the rat liver. *Gene Ther* **17**: 560–564.

27   Fabre, JW, Whitehorne, M, Grehan, A, Sawyer, GJ, Zhang, X, Davenport, M *et al.* (2011). Critical physiological and surgical considerations for hydrodynamic pressurization of individual segments of the pig liver. *Hum Gene Ther* **22**: 879–887.

28   Suda, T, Gao, X, Stolz, DB and Liu, D (2007). Structural impact of hydrodynamic injection on mouse liver. *Gene Ther* **14**: 129–137.

29   Sawyer, GJ, Rela, M, Davenport, M, Whitehorne, M, Zhang, X and Fabre, JW (2009). Hydrodynamic gene delivery to the liver: theoretical and practical issues for clinical application. *Curr Gene Ther* **9**: 128–135.

30   Herweijer, H and Wolff, JA (2007). Gene therapy progress and prospects: hydrodynamic gene delivery. *Gene Ther* **14**: 99–107.

31   Suda, T and Liu, D (2007). Hydrodynamic gene delivery: its principles and applications. *Mol Ther* **15**: 2063–2069.

32   Bonamassa, B, Hai, L and Liu, D (2011). Hydrodynamic gene delivery and its applications in pharmaceutical research. *Pharm Res* **28**: 694–701.

33   Yokoo, T, Kamimura, K, Suda, T, Kanefuji, T, Oda, M, Zhang, G *et al.* (2013). Novel electric power-driven hydrodynamic injection system for gene delivery: safety and efficacy of human factor IX delivery in rats. *Gene Ther* **20**: 816–823.

34   Maruyama, H, Higuchi, N, Nishikawa, Y, Kameda, S, Iino, N, Kazama, JJ *et al.* (2002). High-level expression of naked DNA delivered to rat liver via tail vein injection. *J Gene Med* **4**: 333–341.

35   Sawyer, GJ, Grehan, A, Dong, X, Whitehorne, M, Seddon, M, Shah, AM *et al.* (2008). Low-volume hydrodynamic gene delivery to the rat liver via an isolated segment of

the inferior vena cava: efficiency, cardiovascular response and intrahepatic vascular dynamics. *J Gene Med* **10**: 540–550.

36 Kamimura, K, Suda, T, Zhang, G, Aoyagi, Y and Liu, D (2013). Parameters Affecting Image-guided, Hydrodynamic Gene Delivery to Swine Liver. *Mol Ther Nucleic Acids* **2**: e128.

37 Lecocq, M, Andrianaivo, F, Warnier, MT, Wattiaux-De Coninck, S, Wattiaux, R and Jadot, M (2003). Uptake by mouse liver and intracellular fate of plasmid DNA after a rapid tail vein injection of a small or a large volume. *J Gene Med* **5**: 142–156.

38 Budker, V, Budker, T, Zhang, G, Subbotin, V, Loomis, A and Wolff, JA (2000). Hypothesis: naked plasmid DNA is taken up by cells *in vivo* by a receptor-mediated process. *J Gene Med* **2**: 76–88.

39 Wolff, JA and Budker, V (2005). The mechanism of naked DNA uptake and expression. *Adv Genet* **54**: 3–20.

40 Yeikilis, R, Gal, S, Kopeiko, N, Paizi, M, Pines, M, Braet, F *et al.* (2006). Hydrodynamics based transfection in normal and fibrotic rats. *World J Gastroenterol* **12**: 6149–6155.

41 Kamel, IR, Kruskal, JB, Warmbrand, G, Goldberg, SN, Pomfret, EA and Raptopoulos, V (2001). Accuracy of volumetric measurements after virtual right hepatectomy in potential donors undergoing living adult liver transplantation. *AJR Am J Roentgenol* **176**: 483–487.

42 Lemke, AJ, Brinkmann, MJ, Schott, T, Niehues, SM, Settmacher, U, Neuhaus, P *et al.* (2006). Living donor right liver lobes: preoperative CT volumetric measurement for calculation of intraoperative weight and volume. *Radiology* **240**: 736–742.

Supplementary Information accompanies this paper on the *Molecular Therapy—Methods & Clinical Development* website (http://www.nature.com/mtm)